Machine learning method for real-time non-invasive prediction of individual thermal preference in transient conditions

Andrei Claudiu Cosma and Rahul Simha

Department of Computer Science, School of Engineering and Applied Science, The George Washington University, USA

Abstract

This work introduces a new technique that provides real-time feedback to a Heating, Ventilation, and Air Conditioning (HVAC) system controller with respect to the occupants' thermal preferences to avoid space overheating. We propose a non-invasive approach for automatic prediction of personal thermal comfort and mean time to warm discomfort using machine learning. The prediction framework described uses temperature information extracted from multiple local body parts to model an individual's thermal preference, with sensing measurements that capture local body part variance as well as differences between body parts. We compared the efficacy of using machine learning with classical measurements such as skin temperature along with our approach of using multi-part measurements and derived data. An analysis of the performance of machine learning shows that our method improved the accuracy of personal thermal comfort prediction by an average of 60%, and the accuracy of mean time to warm discomfort prediction by an average of 40%.

The proposed thermal models were tested on subjects' data extracted from an office setup with room temperature varying from low (21.11°C) to high (27.78°C). When all proposed features were used, personal thermal comfort was predicted with an accuracy higher than 80% and mean time to warm discomfort with more than 85% accuracy. Further analysis of the machine learning efficacy showed that temperature differences had the highest impact on performance of individual thermal preference prediction, while the proposed approach was found not sensitive to the actual machine learning algorithm.

Keywords: thermal comfort prediction, feedback technology, thermographic camera, HVAC control, building automation

1 Introduction

Buildings are made for people to work and live in with comfort and satisfaction, and that is why they are at the center of the design process. New constructions are designed to better serve the occupants and to give them a pleasant experience. Human beings are complex, and since a majority of the average person's day is spent indoors (87% of the time [1]), our emotions, well-being, and comfort depend on these environments. For this reason, one important aspect of building design is the indoor environment quality

(IEQ). The National Institute for Occupational Safety and Health (NIOSH) defines the IEQ as "the quality of a building's environment in relation to the health and well-being of those who occupy space within it." The IEQ is determined by the sum of the following individual qualities: vibrations, odors, lighting, sounds, air, and thermal comfort. An improved IEQ can not only enhance the lives of a building's occupants, but will also increase the resale value of the building, and it can, in the case of work environments, affect the productivity of employees.

If the indoor environment is not aligned with the occupants' expectations, occupants will seek new ways to compensate for these inconveniences. For instance, in an office space with insufficient lighting, occupants will seek visual comfort by adding extra table or floor lamps. Similarly, when the office temperature is too low, occupants will seek thermal comfort by employing personal space heaters. However, these corrective actions could cost occupants or put them in conflict with employer policy, can create potential fire and mobility hazards, and almost always will lead to an inefficient use of energy. Therefore, proper space design for occupants' comfort and well-being can also contribute to better energy efficiency and workplace safety.

The Leesman Index from 2017 [2], which assessed how office spaces are supporting employees, specifies that the top ten most important physical features of the working space are dominated by the IEQ, with five out of ten features. After naming "desk" and "chair" as the most important workplace physical features for employees (for 88% and 86% of them), equally important for 80% of them were "small meeting rooms" and "temperature control", followed by "natural light" (75%), "noise levels" (74%), "personal storage" (73%), "large meeting rooms" (70%), "air quality" (70%), and "office lighting" (65%). Also, when employees were asked how satisfied they were with these physical features, only 29% of employees were satisfied with their workplace's "temperature control", 31% with the "noise level", 40% with the "air quality", and 58% with the "office lightning". This study shows that the indoor thermal quality (ITQ), a component of the IEQ, is one of the most important physical features of an office building, but the current average employee satisfaction with respect to this is actually quite low.

Other studies have explored additional implications of ITQ in relation to its impact in the workplace. Sandage et al. [3] focused on the influences of ITQ on vocal comfort and function, van Hoof et al. [4] focused on the special thermal needs for people with disabilities, and Heerwagen [5] reviewed ITQ's impact on the productivity of green buildings' employees. All these studies support the relevance of ITQ, both in office and residential buildings, as well as in health care institutions.

ITQ is driven by the building's heating, ventilation, and air conditioning system (HVAC). Existing HVAC systems can be classified in two groups: environment-based and occupant-centered. Traditional HVAC systems are environment-based, working on a setpoint temperature computed using real-time attributes of the environment where they act (such as air temperature and air humidity) and fixed occupants' attributes (such as clothing insulation and metabolic rate). This approach was developed by Fanger in the 1970s [6] and later was refined in the ASHRAE-55 standards [7]. It is assumed that any building that adopts this standard will be able to keep at least 80% of its occupants comfortable. However, as the Leesman Index and other works [8, 9, 10, 11] revealed, occupants' satisfaction with ITQ was much lower than expected. For example, the 215 office buildings study in [8] showed that only 11% of the studied buildings had at least 80% of the occupants comfortable.

The low occupants' satisfaction with respect to ITQ reflects the limited capabilities of the traditional HVAC system to accommodate the *individual* thermal needs of the occupants. To overcome this issue, an HVAC control system needs to integrate the occupants' individual thermal preferences in real-time. This approach was recently explored and has come to represent *occupant-centered* HVAC systems [12, 13, 14, 15, 16].

Occupants' individual thermal preference could come directly from them using a manually operated online feedback system or a thermostat; or it could be automatically estimated using data from continuously operating sensors. Direct feedback from the occupants based on a web interface or zonal thermostats was used in [12, 13, 14] to adjust the setpoint temperature for a decentralized HVAC operation, which resulted in improvements of occupants' satisfaction and energy use. However, results from [17] showed that there was a significant gap between users' expectations from the local temperature controller and the system designers' perspective on the users' needs.

A second approach that used manual feedback from the occupants assumed the existence of a personal comfort system that the occupant could control for their individual thermal comfort. This approach was slightly different than all the previous ones, since it did not try to adjust a centralized HVAC system:

instead, it used smaller units to compensate for discrepancies between personal preferences and overall space temperature. To achieve this, the approach in [15, 16] proposed retrofitted office furniture with integrated cooling and heating elements. However, there were a few issues with occupants' manual feedback: occupants had to continuously interact with the system, and the feedback was connected to a fixed location, which became inapplicable if the user moved within the building (for example, to a conference room). For these reasons, a more direct approach of automated sensing of individual thermal comfort is advantageous.

Mathematical modeling of individual thermal preference focuses on the quantifiable response of the human body with respect to the environmental thermal conditions, also known as human body thermoregulation. An in depth literature review on thermal comfort modeling presented by Rupp et al. [18] showed an increasing body of work which can be divided in two groups: invasive and non-invasive methods.

With respect to the invasive methods, researchers have focused on extracting skin temperature using sensors attached to the subjects' body. This information was used to model human body thermoregulation [19, 11, 20, 21, 22, 23] as a means to predict comfort. These works concluded that the mean skin temperature collected from multiple body locations (such as arms, torso and head) could model an occupant's thermoregulation, which correlated with the occupant's thermal comfort. Dai et al. [21] used skin temperature differences between the selected body parts to improve thermal comfort prediction, while Choi et al. [23] relied on skin temperature gradient, and Chaudhuri et al. [22] showed that using normalized hand skin temperature based on inter-individual differences (such as clothing insulation and body surface area) could improve prediction of occupants' thermal sensation. However, these methods are harder to use in practice, because temperature sensors used require physical contact with the occupants' skin.

A non-invasive method, but which still requires physical contact with the occupant, was proposed by Ghahramani et al. [24] using retrofitted eyeglasses with point infrared sensors for skin temperature measurement. Using four sensors, the proposed method extracted skin temperature from nose, forehead, right cheek, and left ear to predict thermal comfort. Also, temperature differences between these locations were considered for improved prediction performance.

With respect to the non-invasive contact-less methods, researchers have focused on utilizing thermographic cameras to collect skin temperature and model thermoregulation. Burzo et al. [25] explored using hand-held thermographic cameras and manual measurements of facial temperature and other physiological signals to predict subjects' thermal comfort level. Similarly, Ranjan et al. [26] used a hand-held camera to extract skin temperature from the hands and head to predict cooling or heating demand. Two more recent works have used programmable thermographic cameras to automatically extract skin temperature. Pavlin et al. [27] automatically extracted skin temperature from forehead key-points as a measure of thermal comfort, while Cosma et al. [28] automatically extracted skin and clothing temperature from arms, torso, and head and demonstrated a significant correlation between their temperatures and the subject's thermal comfort.

Based on these preliminary studies [25, 26, 27, 28], we believe that non-invasive technologies based on thermographic cameras can be used to provide real-time feedback of occupants' individual thermal preference to an HVAC system controller to minimize thermal discomfort and inefficient use of energy. In the following sections, we propose a machine learning method for detecting space overheating scenarios based on occupants' individual thermal preferences. The individual thermal preference consists of: (1) personal thermal comfort (PTC), and (2) mean time to warm discomfort (MTWD) measured in transient conditions. While most of the above studies focused mainly on skin temperature, this method, similar to [28], explored both skin and clothing temperature, as well as temperature variance in a small area. Moreover, derived measurements such as temperature differences [21, 24] and temperature gradient [22, 23] were investigated. We ranked all measurements based on their likelihood of improving the classifier's performance, such as accuracy, precision and recall. Finally, we introduced a new thermal model to predict occupant's thermal preference in real-time. We trained and tested the proposed thermal models using the office-based dataset with transient conditions (going from low to high temperatures) introduced in [28].

2 Methods

The proposed method for an occupant-centered HVAC control system automatically predicts individual thermal comfort of the space occupants, as well as the mean time to warm discomfort given the individual's thermal response to the ambient conditions. We believe that an ideal HVAC system non-invasively perceives the building occupancy and the individual thermal preferences of the occupants in real-time, such that the room temperature is continuously adjusted to reflect the real thermal needs of the occupants. For this reason, each change in temperature has to be evaluated on how it will impact each individual. In situations with multiple individuals in a room, the mean time to discomfort can be used to decide between conflicting goals amongst particular individuals, by preferring the controls needed for individuals with a shorter time to discomfort. If such an approach has reasonably high prediction accuracy, future HVAC systems can dynamically adjust heating customized to individuals before a state of discomfort is reached. While the focus of this paper is on warm discomfort, the general principles of non-invasive sensing combined with machine learning are applicable to cold discomfort once a model is developed based on cold discomfort data.

The individual thermal preference model proposed here consists of the predicted personal thermal comfort and mean time to warm discomfort. The prediction framework incorporates skin and clothing temperatures extracted in real-time from different local body parts, such as arms, torso and head, using a non-invasive technology based on thermographic cameras. The main steps of the proposed method are shown in Figure 1 and are described in detail in the following sections.

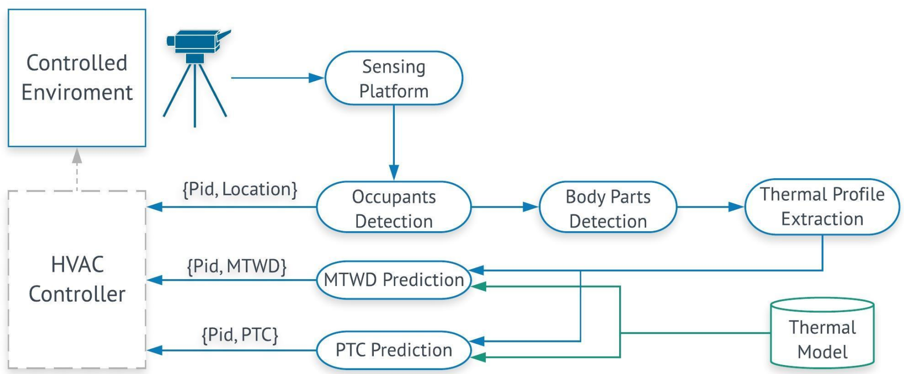

Figure 1: Proposed method for individual thermal preference prediction for an occupant-centered HVAC control system.

2.1 Sensing Platform

The sensing platform used to extract thermal information was introduced by Cosma et al. [28]. This system fuses information from three sensors: a color camera, a depth sensor, and a thermographic camera. The data from all sensors combine to create an augmented representation of the world, called RGB-DT (Red-Green-Blue, Depth, and Temperature). The augmented model was used to detect space occupants and their body parts, from which skin and clothing temperatures were extracted. The benefits of this system are: real-time processing capabilities, non-invasive surface temperature measurement, and low cost hardware.

2.2 Occupants detection and body parts identification

Occupant detection and tracking was performed in the RGB-DT space using the Kinect 2 software. A unique identification number and a precise location was assigned to each detected occupant. Based on the occupant's location, multiple body parts were identified using the neural network framework OpenPose proposed in [29] and freely available on GitHub. Because only upper body parts are likely to be visible and unoccluded by furniture in a typical office settings, the following body parts were selected from which to extract skin and clothing temperature: hand, elbow, shoulder, chest, and head, each of which has been identified to be highly influential for thermal comfort modeling [19, 11, 20, 21, 22, 23, 28]. For each identified body part, its location and type were automatically computed.

2.3 Thermal profile extraction

As defined in previous works [21, 22, 23], the thermal profile of a subject consists of multiple single point skin temperature measurements at different body locations, which are typically recorded with skin-attached temperature sensors. However, some of these body regions, such as the head, were shown to vary significantly in temperature within small areas requiring a higher density of measuring points for proper modeling of the temperature dynamics. In contrast with these approaches, the thermal profile proposed in this paper uses thousands of measuring points on the skin or clothing surface, limited only by the thermographic camera resolution. Since not all skin points are relevant for individual thermal preference prediction, patches were defined around the selected points of interest.

The identified local body parts and the RGB-DT model were used to generate the thermal profile of each subject. The thermal profile consisted of the following two base measurements:

- mean surface temperature (MST): given the location of the local body part, a patch around this location was computed such that all points within the patch were part of the same surface; then, the average temperature was extracted for the patch surface. In contrast with single point temperature measurements, the patch mean temperature is a better representation of the local body temperature, and it is less prone to noise and errors in detection of the local body part location;

- temperature variance ($VarT$): given the face patch area, the temperature variance within the patch was also extracted. As shown in [28], temperature dynamics at the face level changed with the subject's comfort level. If the temperature variance was higher at lower ambient temperatures corresponding to cold discomfort, the patch temperatures homogenized with the increase in the ambient temperature corresponding to warm discomfort. We selected for evaluation the face temperature variance because the analysis on the selected dataset [28] showed that only the face patch temperature variance was significantly ($p < .05$) correlated with thermal comfort.

Also, two derived measurements were identified as relevant for thermal comfort modeling [21, 24, 23, 22, 28] and integrated in the extended thermal profile:

- mean surface temperature gradient (∇MST): the gradient in the patch temperature was computed because, (1) a high gradient denotes an increased thermal stress that may result in thermal discomfort; and (2) the gradient captures the temporal component of the patch temperature, which together with the absolute value of the mean skin temperature are a function of the mean time to discomfort.

$$\nabla MST_t(i, r) = MST_t(i) - MST_{t-\delta}(i) \tag{1}$$

  where i denotes the local body part, t denotes the sampling time, and δ denotes the time interval for gradient calculation. In the proposed experiment, the sampling time is 0.1 seconds and the time interval is 60 seconds.

- mean surface temperature differences (ΔMST): as mentioned in [28], the dynamics between different local body parts was relevant for thermal comfort modeling. It was shown that when thermal comfort changes, temperature differences between two local body parts also change. To model these changes, the mean surface temperature difference between a reference local body part and all other parts was extracted:

$$\Delta MST_t(i) = MST_t(i) - MST_t(r), i \neq r \tag{2}$$

  where i denotes any local body part different than r (the reference local body part), and t denotes the sampling time.

Given the above measurements, the extended thermal profile at a given time is defined as:

$$P_t = \left\{ \begin{array}{lll} MST_t(0), & ... & MST_t(N) \\ VarT_t(f), & & \\ \nabla MST_t(0), & ... & \nabla MST_t(N) \\ \Delta MST_t(0, r), & ... & \Delta MST_t(N-1, r) \end{array} \right\} \tag{3}$$

where N denotes the total number of body parts, f denotes the face patch area, and r denotes the reference local body part used to compute temperature differences. Based on the selected five local body parts the extend thermal profile consists of 15 features.

Finally, there are two types of surfaces that can be detected at different local body part locations:

- skin surface: used to compute mean skin temperature, as proposed in previous works [21, 22, 23].
- clothing surface: in the context of non-invasive technologies, such as thermographic cameras, the skin is not always visible; however underneath each clothing layer is a skin layer that will affect the clothing temperature which has no temperature of itself. So, considering a thin layer of clothing (clothing insulation ≤ 1 clo), the heat exchange between the air temperature and skin temperature through the clothing layer is modeled as an indicator of thermal comfort. As discussed in [28], clothing layers tend to reflect the room temperature when human body heat transfer is low (equivalent of cold discomfort), while they reflect human body temperature when human body heat transfer is high (equivalent of warm discomfort).

2.4 Thermal model and prediction framework

Our thermal model was learned using the thermal profile of all identified local body parts (P_t). The proposed thermal model was trained to predict occupants' individual thermal preference, such as personal thermal comfort and mean time to warm discomfort. Individual classifiers were trained for the two tasks. The training process is explained in detail in the following sections.

2.4.1 Personal thermal comfort prediction

To predict the personal thermal comfort of the occupant, a multi-class classifier was trained based on the extended thermal profile. The subjects' feedback with respect to the thermal comfort vote (TCV) was used as label for the extracted thermal profiles used in the supervised learning framework. Although subjects rated their thermal comfort based on a five-point scale TCV (see Section 3), a three class classifier was trained based on comfort, cold discomfort, and warm discomfort levels. High cold and warm discomfort levels were discarded for this experiment because these situations should never occur in heated, ventilated, and air conditioned buildings [30]. This is also supported by the used dataset where there were no subjects filling high cold discomfort and only six felt high warm discomfort for less than three minutes, while the room temperature varied between 21.11°C and 27.78°C. Classifying comfort and cold/warm discomfort is a more difficult task because the boundary between classes is much narrower. Moreover, the comfort and cold/warm discomfort classification is an important step in optimizing HVAC functionality to better assess the occupants' individual thermal preference. However, if high cold and warm discomfort are important in certain scenarios, the proposed framework can be extended to accommodate the two extra classes by training a new classifier with five classes.

Finally, given that the subject feedback was collected once per minute and data frames were collected at nine frames per second, multiple frames around each individual feedback were used to generate a single thermal profile. To achieve this, a one minute window was centered at the feedback's collection time (30 seconds before and after the feedback), and all thermal profiles within this window were used to compute a polynomial function that estimates the best thermal response.

2.4.2 Mean time to warm discomfort prediction

Similar to the personal thermal comfort prediction, a multi-class classifier was trained to predict mean time to warm discomfort. The following classes were considered: 0 (warm discomfort), (between 1 and 10 minute to warm discomfort), 10+ (more than 10 minutes to warm discomfort). The reasons for using these class labels are as follow: label 0 is for subjects that are already feeling warm discomfort and suggests immediate action rather than prediction of time to discomfort; label 10 is for subjects approaching warm discomfort that can be kept comfortable if immediate action is taken; and label 10+ is for subjects far from warm discomfort where no actions are needed.

Class labels were automatically generated based on the subjects' feedback, such that if the subject was comfortable (TCV=0) with the space temperature and the closest warm discomfort feedback (TCV>0) was less than M minutes away, then the assigned class label is M, where $M \in \{10, \infty\}$. The following equation was used to define the label for each data sample:

$$Label_t = \begin{cases} 0, & \text{if } TCV_t > 0 \\ 10, & \text{if } TCV_t = 0 \text{ and } \exists\delta \text{ with } 0 < \delta \leq 10 \text{ and } TCV_{t+\delta} > 0 \\ 10+, & \text{otherwise} \end{cases} \tag{4}$$

where TCV_t denotes the subject's feedback (thermal comfort vote) at time t and δ denotes the time difference in minutes between two responses.

2.4.3 Feature sets

To train the thermal model classifiers, we used a set of features slightly different from previous works [11, 19, 20, 21] customized for the non-invasive technology. This set of features was based on the extended thermal profile proposed in Section 2.3. To analyze the benefits of different components of the proposed thermal profile, multiple feature sets were defined:

- classical feature set (SkinOnly): consisted of mean skin temperature of head, elbow, and hand. This feature set represents the information used by the previous work.
- base feature set (Base): consisted of mean skin temperatures, where skin is visible, and mean clothing temperatures for clothing covered local body parts;
- temperature variance feature set (BaseVar): consisted of the base feature set plus the temperature variance inside face patch area;
- temperature difference feature set (BaseDiff): consisted of the base feature set plus the temperature difference between reference and all other local body parts;
- temperature gradient feature set (BaseGrad): consisted of the base feature set plus temperature gradient inside each patch area;
- full thermal profile (All): consisted of all proposed features;

For each of these feature sets, a different thermal model was learned and tested using the same sample data. A detailed comparison is presented in Section 4.

2.4.4 Classifiers

Classifier training and testing was performed in Python using the Scikit-learn library. Four classifiers were used to asses the utility of the selected features to predict personal thermal comfort and mean time to warm discomfort: support vector machine (SVM), Gaussian process classifier (GPC), k-neighbors classifier (KNC) and random forest classifier (RFC). Optimal parameters for each model were computed using a grid search technique and kept constant for all tests.

3 Dataset

To train and test the proposed prediction framework, the dataset introduced in [28] was used. This was based on a real scenario, such as an office setup, where temperatures were manipulated and the thermal comfort vote of the occupants was recorded. The office room was located in the middle of the building and had no windows or exterior walls, and was disconnected from the main HVAC unit such that the heating and cooling was controlled locally.

The dataset consisted of 24 healthy subjects, 13 females and 11 males, individually recorded for 27 minutes. All subjects were exposed to identical transient conditions, with the room temperature changing from low (21.11°C) at the beginning of the experiment, to high (27.78°C) by the end of the experiment. The air flow was less than 0.2 m/s, as recommended by ASHRAE-55 [7]. Indoor conditions were continuously monitored by measuring the air temperature and relative humidity in the immediate vicinity of the subject. Based on the logged measurements, the relative humidity was approximately 39% at the beginning of the experiment, and slightly lower at approximately 33% by the end of the experiment. The decrease in relative humidity was the result of using room heaters, which dried the air with approximately 6%. This average trend was observed during data collection on all subjects. In this case we can define relative humidity using a linear function of time and independent of the occupant's thermal comfort. Because of this direct predictability, the relative humidity will not have a significant impact on the prediction results since machine learning algorithms easily account for linearity.

During the experiment, the following parameters were kept constant:

- clothing insulation: all subject were asked to wear a similar outfit (average clothing index was 0.44 clo with SD = 0.07 clo)
- metabolic rate: sedentary office activity (1-1.1 met)

The dataset had more than 350 000 RGB-DT frames recorded at nine frames per second. All frames were processed and thermal profiles were generated at one minute intervals, corresponding to subjects' feedback frequency, such that for each feedback provided (TCV) there was an associated thermal profile. As mentioned in the original dataset's manuscript [28], there were 24 subjects with valid data and each subject provided in total 27 feedbacks with respect to their personal thermal comfort, resulting in 648 data samples (thermal profile plus TCV). Because skin and clothing temperatures were extracted continuously from the RGB-DT frames and feedback was provided only every other minute, we used a sliding window approach to compute the thermal profile. Within the defined time window, we fitted a polynomial function to all the temperature measurements of a body part. Using these polynomial functions, we extracted the instantaneous skin and clothing temperatures corresponding to the given feedback. This approach ensured a reduced observational error.

Subject feedback consisted of the thermal comfort vote on a five-point scale, as defined in [28]: (-2) high cold discomfort, (-1) cold discomfort, (0) comfortable, (+1) warm discomfort, and (+2) high warm discomfort. However, as mentioned in Section 2.4.2 only three classes were used in the prediction framework: (-1) cold discomfort, (0) comfortable, and (+1) warm discomfort. These values were used in the supervised learning framework as class labels to the associated thermal profiles.

We computed the subjects' feedback distribution with respect to the three proposed classes. Results showed that comfortable and warm discomfort classes were well represented, with 288 feedbacks and 276 respectively. However, cold discomfort class was less represented with 44 feedbacks. The dataset unbalance has to be corrected during the training process by weighting more the data samples of the less represented class (cold discomfort). It is worth mentioning that the other 40 feedbacks to the total of 648 was represented by the high warm discomfort, and their were no high cold discomfort feedbacks.

4 Results

Out of the 24 subjects, 20 subjects were randomly selected for training the classifier, while the remaining 4 subjects were used for testing. Separate thermal models were trained based on the feature sets proposed. Classifiers' parameters were chosen at the beginning of the experiment using the "All" feature vector and a grid search technique, and were kept constant for the entire experiment. Also, if not otherwise specified by the test, the complete feature set "All" was used for all of the following tests.

The sections below analyze the trained thermal models from three main perspectives: data overfitting, classifier performance based on multiple classification frameworks, and classifier performance based on different feature sets. Thermal models were also individually analyzed for the two main tasks: predicting personal thermal comfort and mean time to warm discomfort.

4.1 Personal thermal comfort prediction

4.1.1 Overfitting test

To demonstrate the generalization power of the proposed learning framework, a model validation was conducted using a non-exhaustive k-fold cross-validation with 5-folds. Only training samples were used for this test and a compensation for the unbalanced nature of the generated data was applied. All four proposed classifiers were tested and the results are shown in Figure 2. It can be seen that all classifiers performed consistently well across the 5-folds, with both precision and recall approximately equal to 80%. Also, on average all classifiers exceeded 80% precision and recall.

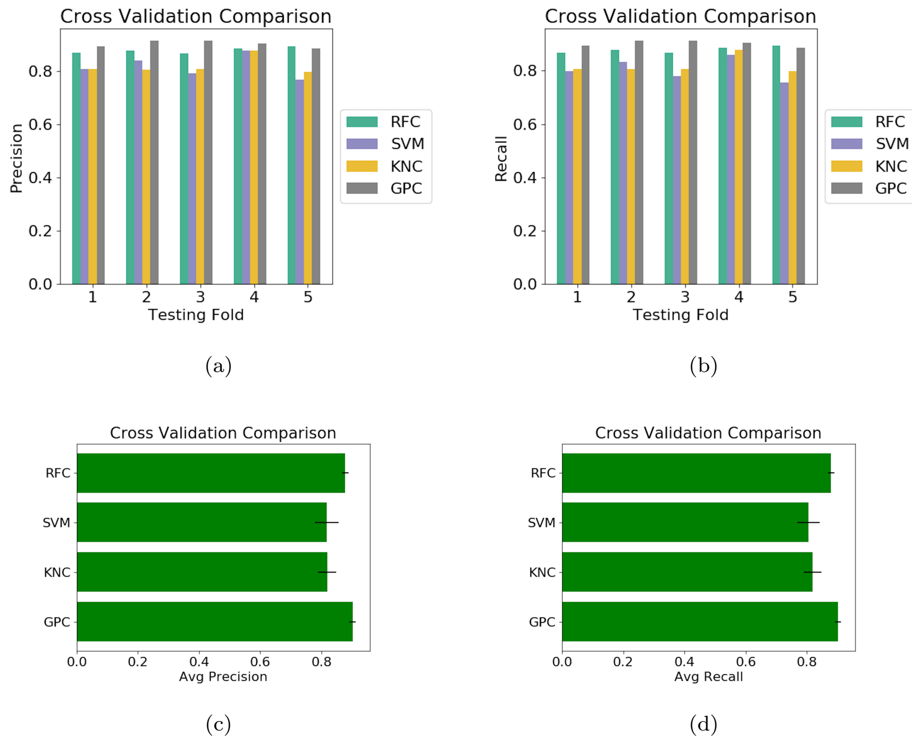

Figure 2: Personal thermal comfort prediction cross-validation with 5-folds: (a) classifiers' precision for each fold, (b) classifiers' recall for each fold, (c) classifiers' average precision over all folds, and (d) classifiers' average recall over all folds.

4.1.2 Classifiers comparison

For the first comparison test, the classifiers' performances were analyzed by comparing how they performed with respect to each of the three proposed classes: comfort, cold discomfort, and warm discomfort. Individual thermal models were learned for each classifier using the "All" feature vector and the samples training set. Next, the confusion matrix was computed for each classifier using the samples testing set. The results are shown in Figure 3.

Based on the confusion matrices, one of the hardest classes to classify was cold discomfort. In the worst case scenario, 33% of the cold discomfort samples where misclassified as comfort, while in the best case scenario all of them were correctly classified. These results could be explained by the fact that there was a smaller number of cold discomfort samples, creating an d dataset that affected the learning process, even though compensation was attempted by weighting the cold discomfort samples more. Also, the lowest

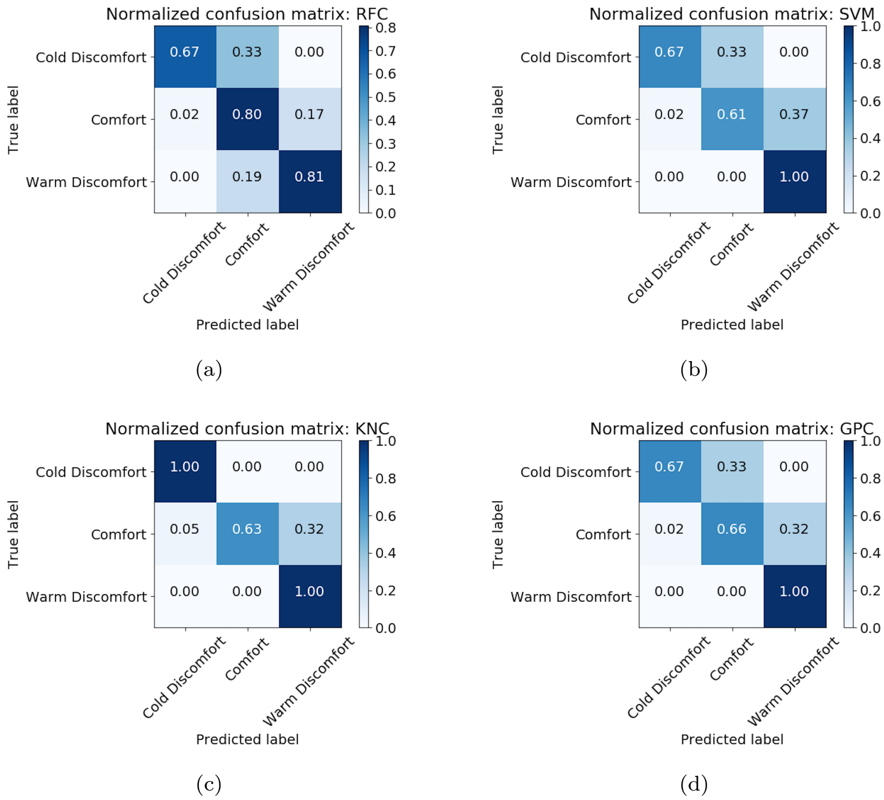

Figure 3: Personal thermal comfort prediction confusion matrix for the three predicted classes, using: (a) RFC, (b) SVM, (c) KNC, and (d) GPC classifiers.

temperature in the office room (21.11°C) was close to the comfort boundary, a limitation of the experimental set up, making the classification at the cold-comfort boundary imprecise. It is expected that if the start room temperature would have been set lower (e.g. 19°C), the new samples collected would be classified correctly, improving the percentage of correctly classified samples.

Three out of four classifiers identified correctly all warm discomfort samples, while the fourth classifier identified 81% of them. The high warm discomfort sensitivity (or recall) impacted the thermal comfortable samples classification by consistently mislabeling 30% of them as warm discomfort. This can be explained by our learning process using the unbalanced dataset with compensation weights for each class, which forced the class separation boundaries to benefit the less represented classes. However, the RFC classifier identified correctly 80% of thermal comfortable samples.

For the second comparison test, the average accuracy, precision, and recall for each classifier were compared. The results are presented in Table 1. Results show that the average accuracy for all the proposed classifiers was close in value at approximately 80% with SD=1.7%. This supports the previous results, which concluded that the thermal model outcome is not purely random. However, this makes the classifier selection less relevant. For this reason, precision and recall values were analyzed to better understand the classifiers' performance.

Based on the classifiers' precision, the KNC and GPC classifiers would misclassify only 14 occupants as comfortable, from an office with 100 occupants, while the other two classifiers would misclassify around 18 occupants as comfortable, with all other occupants correctly classified. Based on the classifiers' recall, three out of four classifiers (KNC, GPC, and RFC) mislabel less than 20 occupants as comfortable from a room with 100 comfortable occupants, while the SVM classifier mislabel less than 24.

To conclude, the classifier selection depends on the final application. If the main purpose is to save

Table 1: Classifiers' average performances using test data for personal thermal comfort prediction.

Classifier	Accuracy	Precision	Recall
SVM	76.0	82.0	76.0
KNC	80.0	86.0	80.0
GPC	80.0	85.0	80.0
RFC	80.0	80.0	80.0

energy, then a classifier with high recall is preferred, such as KNC, GPC or RFC. These ensure that all comfortable occupants are identified. However, if the end application needs a strict control of the occupants' thermal comfort, then a classier with high precision should be selected, such as KNC or GPC. Finally, for applications with mixed requirements, the RFC classifier gives the best overall performances with a well balanced confusion matrix.

4.1.3 Feature sets comparison

This test evaluated the benefits of the different feature sets proposed in Section 2.4.3 in contrast with a reference approach which used only skin temperature. The same four classifiers were used to learn individual thermal models for each of the proposed feature sets. Then, their average accuracy, precision, and recall were computed using the testing samples. Results are shown in Figure 4.

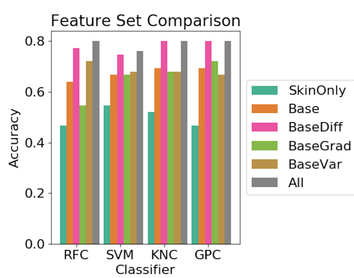

(a)

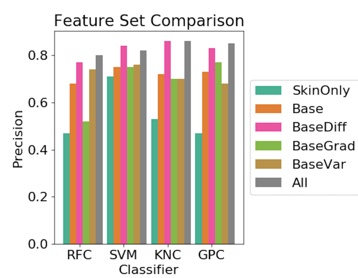

(b)

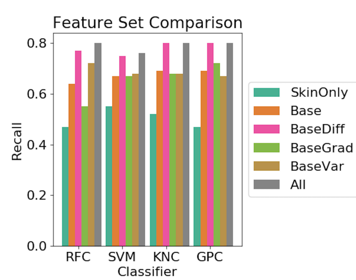

(c)

Figure 4: Proposed feature set performance evaluation for personal thermal comfort prediction: (a) accuracy, (b) precision, and (c) recall.

The reference feature set ("SkinOnly") consisted of skin only temperature readings at the selected local body parts (such as hand, elbow, and head). When an extended feature set was used, the performance was significantly higher for all classifiers with an increase of at least 15% in accuracy, 10% in precision, and 20% in recall. The highest performance jump was achieved when the "All" extended feature set was used. This performance increase was expected, given that the statistical analysis in [28] showed a significant correlation between thermal comfort and the temperature differences and face temperature variance. Although, to better understand the performance increase from the extended features, the accuracy, precision, and recall increase was quantified as a percentage of the reference feature set. These results are presented in Table 2 as an aggregate over all tested classifiers.

Table 2: Performance increase from the extended feature sets with respect to the "SkinOnly" feature set, over all tested classifiers on personal thermal comfort prediction.

Feature Set	Accuracy			Precision			Recall		
	Average	Min	Max	Average	Min	Max	Average	Min	Max
Base	35.2	21.9	48.5	35.3	5.6	55.3	34.3	21.8	46.8
BaseDiff	56.9	36.6	71.4	55.2	18.3	76.6	56.1	36.4	70.2
BaseGrad	31.1	17.2	35.3	28.04	5.7	63.9	30.7	17.0	53.2
BaseVar	38.1	24.4	54.3	35.3	7.1	57.5	37.5	23.6	53.2
All	59.0	39.0	71.5	57.2	15.5	80.9	58.1	38.2	70.2

Based on the percentage of performance improvement, adding clothing temperatures to the reference feature set helped the classifiers' performances increase an average of 35.2% in accuracy, 35.5% in precision, and 34.3% in recall. Since a non-invasive technology has limited access to skin temperatures, this result proves that other observable information, such as clothing temperature, could be used to improve the prediction of personal thermal comfort. Moreover, the highest impact on the accuracy comes from features resulting from temperature differences, with an average increase of 56.9% that can go up to 71.4% for some classifiers. Face temperature variance also significantly increased the accuracy with an average of 38.1%. Based on the precision improvements, temperature differences produced the highest impact with an average increase of 55.2%, followed by face temperature variance with an increase of 35.3%. Furthermore, for some classifiers, the precision increase can go up to 76.6%. Finally, the recall was also improved most by the temperature differences, with an average increase of 56.1%, and a peak increase of 70.2% for some classifiers.

These results indicate that the temperature dynamics between different local body parts changes with the thermal comfort vote. In other words, the temperature of the thin clothing layer is closer to the body temperature when the body heat transfer is high, and is closer to the air temperature when the body heat transfer is low. Also, the results show that face temperature variance is significant for thermal comfort prediction, with high variances when the subjects are uncomfortable and low variances at thermal comfort. Overall, the proposed extended thermal profile improved the classifier performance with up to 71.5% in accuracy, 80.9% in precision, and 70.2% in recall.

The results also show that the temperature gradient had a positive impact for some classifiers, such as SVM and RFC, and a quality degradation for others, such as KNC and GPC. It should be noted that the mean skin temperature gradient would be more relevant in a less structured environment, where temperatures inside the room vary randomly. Also, tasks that require a temporal integration, such as mean time to discomfort, would benefit more from these features.

When all the proposed features ("All") are used, the classifier performances improved the most with an average of 59.0% in accuracy, 57.2% in precision, and 58.1% in recall. The improvement was similar with the performance obtained by temperature differences. This result shows that there is an overlap between the proposed features, but each of them explains a small amount of individual variance within the predicted classes.

4.2 Mean time to warm discomfort prediction

4.2.1 Overfitting test

The non-exhaustive cross-validation experiment for testing thermal model generalization power was repeated for the mean time to warm discomfort classifiers. The results are shown in Figure 5.

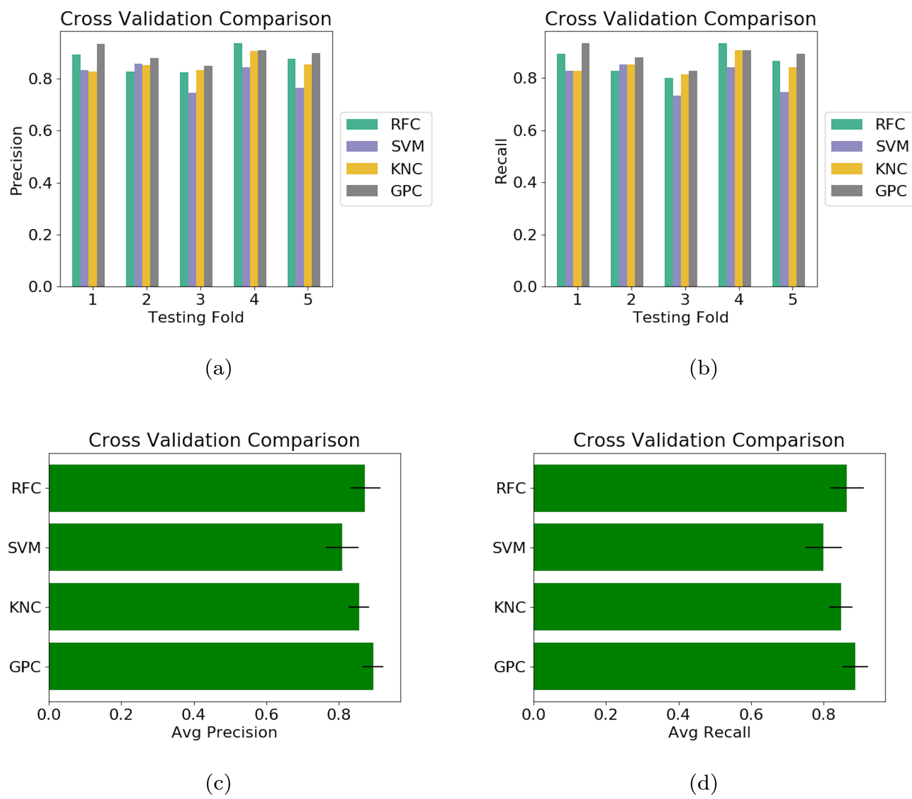

Figure 5: Mean time to warm discomfort prediction cross-validation with 5-folds: (a) classifier precision for each fold, (b) classifier recall for each fold, (c) classifier average precision over all folds, and (d) classifier average recall over all folds.

The classifiers' performances were constant across the 5-folds, with precision and recall values between 80% and 85%. Also, it can be observed that the more difficult bins to classify, such as bin three, impacted all classifier results, while the easier bins to classify, such as bin four, elevated all classifier results. This classifier homogeneity reinforces the generalization power of the chosen model.

4.2.2 Classifier comparison

The same procedure as described in Section 4.1.2 was followed to compare classifier performances. First, the confusion matrix for the four proposed classes was computed for each classifier. Results are shown in Figure 6.

Based on the confusion matrices, the hardest class to predict was the "10" minutes to warm discomfort class. The lowest performance classifier (GPC) misclassified 36% of the warm discomfort samples as "0" minutes away from warm discomfort and 5% as "10+" minutes to warm discomfort. The best classifier (SVM) misclassified only 27% of the samples as "0" minutes away from warm discomfort. The observed consistent misclassification between "0" and "10" minutes to warm discomfort classes is associated with the

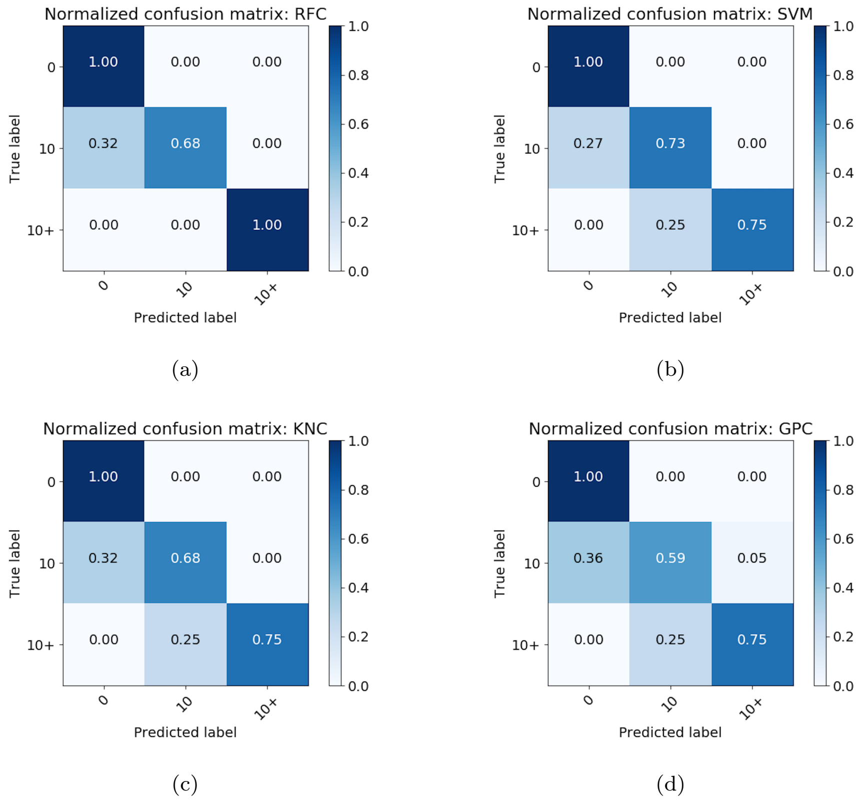

Figure 6: Mean time to warm discomfort prediction confusion matrix for the four predicted classes, using: (a) RFC, (b) SVM, (c) KNC, and (d) GPC classifiers.

subjective nature of the thermal comfort, which makes the transition between the two states a non-binary decision. The "0" minutes to warm discomfort class was consistent correctly identified in 100% of the cases. The "10+" minutes to warm discomfort class was correctly identified in at least 75% of the cases, with a consistent overlap with class "10". The overlap is explained by the fact that these classes represent two subgroups of the thermal comfortable samples.

Given that the correctly classified samples are represented by the numbers on the principal diagonal of the confusion matrix, and all other cells represent misclassified samples, it can be observed that values below the principal diagonal are higher than the ones above the diagonal. This translates to an underestimation of the time to warm discomfort, with subjects being actually farther away from warm discomfort than predicted. This is the preferred scenario for situations where warm discomfort is not acceptable, ensuring that subjects never reach a state of warm discomfort to begin with. However, in situations where is preferred the overestimations of mean time to warm discomfort, the classifiers have to be retrained with a higher weight for the last two classes ("10" and "10+").

Next, the classifier average accuracy, precision, and recall on the testing samples were compared. The results are shown in the Table 3. The highest performances were achieved by the RFC and SVM classifiers with the highest value on all three average metrics (87.7% - 90.0% - 88.0%). These were closely followed by the KNC classifier, but the former ones had a minimal performance advantage (on average 2% more). The GPC classifier had marginally lower performances, with an average accuracy of 82.5%, precision of 84%, and recall of 82%.

To conclude, predicting mean time to warm discomfort in uniform transient conditions can be done very accurately (>87%) when the SVM classifier and the extended feature set are used. However, if the "10" and "10+" minutes to warm discomfort classes are of higher importance, then RFC classifier provide a more

Table 3: Classifier average performances using test data for mean time to warm discomfort prediction.

Classifier	Accuracy	Precision	Recall
SVM	87.7	89.0	88.0
KNC	86.0	88.0	86.0
GPC	82.5	84.0	82.0
RFC	87.7	90.0	88.0

accurate classification of these two.

4.2.3 Feature set comparison

The proposed feature sets (see Section 2.4.3) and the reference feature set ("SkinOnly") were compared to better understand how they improve the task of predicting mean time to warm discomfort. The individually trained thermal models were compared based on their accuracy, precision, and recall obtained on the testing samples. Results are shown in Figure 7.

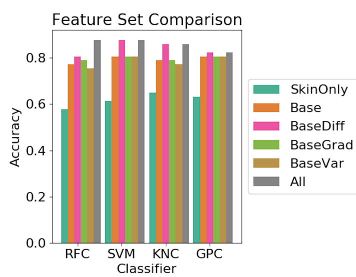

(a)

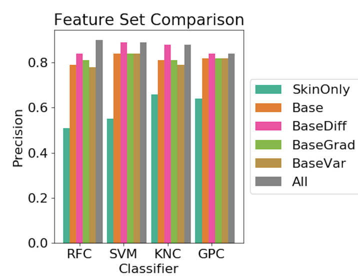

(b)

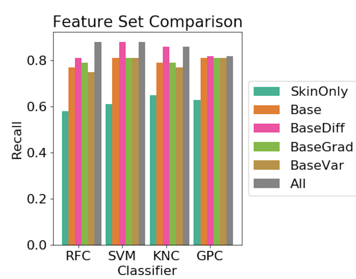

(c)

Figure 7: Proposed feature set performance evaluation for mean time to warm discomfort prediction: (a) accuracy, (b) precision, and (c) recall.

It can be observed that the reference feature set performs fairly well, with approximately 60% accuracy, precision, and recall. However, if any of the proposed feature sets was used, all classifier performances were improved significantly. The overall highest performance was achieved when the "All" feature set and the RFC or SVM classifier were used. This was expected given that more relevant information was available to the classifier to distinguish between classes. Furthermore, all proposed classifiers had comparable performances. To better understand the performance increase generated by the extended feature sets, the average/min/max performance increase of all classifiers with respect to the reference feature set was studied. The results are shown in Table 4.

Table 4: Performance increase from the extended feature sets with respect to the base feature set, over all tested classifiers on mean time to warm discomfort prediction.

Feature Set	Accuracy			Precision			Recall		
	Average	Min	Max	Average	Min	Max	Average	Min	Max
Base	28.5	21.6	33.3	39.6	22.7	54.9	28.9	21.5	32.7
BaseDiff	36.3	30.6	42.9	47.8	31.3	64.7	36.6	30.2	44.3
BaseGrad	29.3	21.6	36.4	40.6	22.7	58.8	29.8	21.5	36.2
BaseVar	27.2	19.0	31.4	38.4	19.7	53.0	27.3	18.5	32.8
All	39.4	30.6	51.5	50.8	31.3	76.5	39.6	30.2	51.8

These results show that the proposed clothing temperatures helped improve mean time to warm discomfort prediction with more than 28% accuracy, 39% precision and 28% recall. This supports again the importance of using all observable information, when access to skin temperature data is limited. The temperature differences had the highest impact on mean time to warm discomfort prediction. On average, the "BaseDiff" feature set increased the accuracy by 36.3%, precision by 47.8%, and recall by 36.6%. Also, this extended feature set had the highest performance increase in the worst (min) and best (max) case scenario. Similar to personal thermal comfort prediction, the "All" feature set obtained the highest performance increase. However, in the worst case scenario the "All" feature set performance is identical with the "BaseDiff" feature set. This observation shows that for some classifiers when the temperature differences are used, the temperature variance and gradient do not provide the classifier with extra information that could help the classifier solve the failure scenarios.

The temporal integration of the temperature represented by the temperature gradient, increased the overall classifier performances by more than 29% for all studied metrics. Moreover, it can be observed that the temperature gradient impact was more significant in the case of mean time to warm discomfort, than it was for thermal comfort prediction. This can be explained by the fact that a near constant gradient did not affect the personal thermal comfort of the occupant, but gave important information about how soon skin temperature will reach the warm discomfort state.

5 Conclusion

We proposed a real-time machine learning method for individual thermal preference prediction in transient conditions to avoid space overheating. At the core of the system is an innovative, non-invasive, and contactless technique that is capable of accurately predicting personal thermal comfort of the space occupants, as well as mean time to warm discomfort if the occupant is thermally comfortable. To the best of our knowledge, this is the first work to investigate a machine learning method to predict the mean time to thermal discomfort of an occupant. The prediction framework was based on a mathematical modeling of human body thermoregulation observed in an office setup with uniform transient conditions.

Occupant thermal profiles were automatically extracted from the RGB-DT model proposed in [28]. Similar to the classical approaches to model thermal comfort, the thermal profile definition consisted of skin temperatures at different local body locations such as the arms and head. However, the proposed definition also included clothing temperature, temperature gradient, temperature variance inside the patch area, and temperature differences between different body sampling locations. Furthermore, the proposed thermal model could be extended in the future to integrate real-time measurements of the environment attributes, such as relative humidity and radiant temperature. When compared with the skin only thermal profile, the proposed thermal profile improved the prediction accuracy of personal thermal comfort by more than 60% on average and up to 71% in some scenarios, and mean time to warm discomfort by 40% on average and up to 51% in some scenarios.

Multiple feature sets were proposed and tested based on the extended thermal profile. Features such as temperature differences appeared to improve the most personal thermal comfort prediction, as well as mean time to warm discomfort. Face temperature variance appeared to be more relevant for personal thermal comfort classification, while temperature gradient was more significant for mean time to warm discomfort prediction. These findings indicate that the signal needed for thermal comfort discrimination is spread across multiple features since classification with the full set of features is superior to that when using subsets, suggesting that the personal experience of discomfort results in a multitude of observable effects on various parts of the skin. All these results support the statement that temperature dynamics change with thermal comfort level. However, features such as clothing temperature and temperature differences depend on the thickness of the clothing layer, which was kept constant in the dataset used. For this reason, it would be useful to conduct multiple experiments in the future to understand how different clothing insulation affect clothing temperature.

The proposed thermal models were trained and tested on the RGB-DT dataset proposed in [28]. While this experiment reflects a real office scenario with transient conditions, a drawback was that the temperature inside the office increased at a constant rate for all subjects. In different scenarios, room temperatures can vary non-uniformly, which could affect the mean time to warm discomfort prediction. For this reason, it would be useful to conduct multiple experiments in the future, where different transient conditions are tested, to understand if a single thermal model could be used with mixed transient conditions.

We also introduced a complete processing pipeline for real-time prediction of individual thermal preference. A key finding is that our approach was not sensitive to the actual machine learning algorithm, suggesting that the proposed model is sufficient for a generic machine learning technique. Using this method, personal thermal comfort was predicted with more than 80% accuracy, while mean time to warm discomfort was predicted with more than 85% accuracy. Although, with respect to personal thermal comfort prediction, cold discomfort was harder to classify due to a limited number of samples in this class. Also, with respect to mean time to warm discomfort, “0” and “10” minutes to warm discomfort were harder to separate with a binary decision due to a fuzzy transition between the thermal comfort and warm discomfort states.

Occupant-centered HVAC control systems are part of a new generation of intelligent heating and cooling systems, with a focus on personal thermal comfort and energy efficiency. These systems will learn how to respond to the occupants’ thermal needs and how to schedule the HVAC system on and off time such that most occupants will remain thermally comfortable while improving energy efficiency. Further research is required to develop HVAC control systems capable of using the thermal comfort feedback from a system like this in real-time, and to produce an occupant-centered schedule of heating and air conditioning.

References

[1] N. E. Klepeis, W. C. Nelson, W. R. Ott, J. P. Robison, A. M. Tsang, P. Switzer, J. V. Behar, S. C. Hern, W. H. Engelmann, The national human activity pattern survey (nhaps): a resource for assessing exposure to environmental pollutants, Journal Of Exposure Analysis And Environmental Epidemiology 11.
URL `http://dx.doi.org/10.1038/sj.jea.7500165`

[2] N. Risner, C. Murray, P. Rothe, A briefing on global workplace strategy, management, satisfaction and effectiveness, The Leesman Review.

[3] M. J. Sandage, K. A. Rahn, A. G. Smith, Vocal ergonomics in the workplace: Heating, ventilation, and air-conditioning method influences on vocal comfort and function, Journal of Speech, Language, and Hearing Research 60 (2) (2017) 355–363. `doi:10.1044/2016_JSLHR-S-16-0081`.
URL `+http://dx.doi.org/10.1044/2016_JSLHR-S-16-0081`

[4] J. van Hoof, H. Kort, J. Hensen, M. Duijnstee, P. Rutten, Thermal comfort and the integrated design of homes for older people with dementia, Building and Environment 45 (2) (2010) 358 – 370, 1st Inter-

national Symposium on Sustainable Healthy Buildings. doi:https://doi.org/10.1016/j.buildenv.2009.06.013.
URL http://www.sciencedirect.com/science/article/pii/S0360132309001565

[5] J. Heerwagen, Green buildings, organizational success and occupant productivity, Building Research & Information 28 (5-6) (2000) 353–367. arXiv:https://doi.org/10.1080/096132100418500, doi:10.1080/096132100418500.
URL https://doi.org/10.1080/096132100418500

[6] P. O. Fanger, Thermal comfort: Analysis and applications in environmental engineering, Danish Technical Press, 1970.
URL https://books.google.com/books?id=S0FSAAAAMAAJ

[7] ASHRAE, ANSI/ASHRAE Standard 55: Thermal Environmental Conditions for Human Occupancy, American Society of Heating, Refrigerating and Air Conditioning Engineers, Atlanta, Georgia, 2013.

[8] C. Huizenga, S. Abbaszadeh, L. Zagreus, E. A. Arens, Air quality and thermal comfort in office buildings: results of a large indoor environmental quality survey, Proceedings of Healthy Buildings III (2006) 393–397.

[9] J. V. Hoof, Forty years of fanger's model of thermal comfort: comfort for all?, Indoor Air 18 (3) (2007) 182–201. arXiv:https://onlinelibrary.wiley.com/doi/pdf/10.1111/j.1600-0668.2007.00516.x, doi:10.1111/j.1600-0668.2007.00516.x.
URL https://onlinelibrary.wiley.com/doi/abs/10.1111/j.1600-0668.2007.00516.x

[10] M. Fountain, G. Brager, R. de Dear, Expectations of indoor climate control, Energy and Buildings 24 (3) (1996) 179 – 182. doi:https://doi.org/10.1016/S0378-7788(96)00988-7.
URL http://www.sciencedirect.com/science/article/pii/S0378778896009887

[11] W. Liu, Z. Lian, Q. Deng, Y. Liu, Evaluation of calculation methods of mean skin temperature for use in thermal comfort study, Building and Environment 46 (2) (2011) 478 – 488. doi:https://doi.org/10.1016/j.buildenv.2010.08.011.
URL http://www.sciencedirect.com/science/article/pii/S0360132310002647

[12] F. Jazizadeh, F. M. Marin, B. Becerik-Gerber, A thermal preference scale for personalized comfort profile identification via participatory sensing, Building and Environment 68 (2013) 140 – 149. doi:https://doi.org/10.1016/j.buildenv.2013.06.011.
URL http://www.sciencedirect.com/science/article/pii/S0360132313001893

[13] F. Jazizadeh, A. mani, B. Becerik-Gerber, T. Kichkaylo, M. Orosz, User-led decentralized thermal comfort driven hvac operations for improved efficiency in office buildings, Energy and Buildings 70 (2014) 398 – 410. doi:https://doi.org/10.1016/j.enbuild.2013.11.066.
URL http://www.sciencedirect.com/science/article/pii/S0378778813007731

[14] B. Balaji, H. Teraoka, R. Gupta, Y. Agarwal, Zonepac: Zonal power estimation and control via hvac metering and occupant feedback, in: Proceedings of the 5th ACM Workshop on Embedded Systems For Energy-Efficient Buildings, BuildSys'13, ACM, New York, NY, USA, 2013, pp. 18:1–18:8. doi:10.1145/2528282.2528304.
URL http://doi.acm.org/10.1145/2528282.2528304

[15] H. Zhang, E. Arens, M. Taub, D. Dickerhoff, F. Bauman, M. Fountain, W. Pasut, D. Fannon, Y. Zhai, M. Pigman, Using footwarmers in offices for thermal comfort and energy savings, Energy and Buildings 104 (2015) 233 – 243. doi:https://doi.org/10.1016/j.enbuild.2015.06.086.
URL http://www.sciencedirect.com/science/article/pii/S0378778815301067

[16] W. Pasut, H. Zhang, E. Arens, Y. Zhai, Energy-efficient comfort with a heated/cooled chair: Results from human subject tests, Building and Environment 84 (2015) 10 – 21. doi:https://doi.org/10.1016/j.buildenv.2014.10.026.
URL http://www.sciencedirect.com/science/article/pii/S0360132314003473

[17] S. Karjalainen, O. Koistinen, User problems with individual temperature control in offices, Building and Environment 42 (8) (2007) 2880 – 2887. doi:https://doi.org/10.1016/j.buildenv.2006.10.031.
URL http://www.sciencedirect.com/science/article/pii/S0360132306003349

[18] R. F. Rupp, N. G. Vasquez, R. Lamberts, A review of human thermal comfort in the built environment, Energy and Buildings 105 (2015) 178 – 205. doi:https://doi.org/10.1016/j.enbuild.2015.07.047.
URL http://www.sciencedirect.com/science/article/pii/S0378778815301638

[19] J.-H. Choi, V. Loftness, Investigation of human body skin temperatures as a bio-signal to indicate overall thermal sensations, Building and Environment 58 (2012) 258 – 269. doi:https://doi.org/10.1016/j.buildenv.2012.07.003.

[20] Q. Jin, X. Li, L. Duanmu, H. Shu, Y. Sun, Q. Ding, Predictive model of local and overall thermal sensations for non-uniform environments, Building and Environment 51 (2012) 330 – 344. doi:https://doi.org/10.1016/j.buildenv.2011.12.005.
URL http://www.sciencedirect.com/science/article/pii/S0360132311004215

[21] C. Dai, H. Zhang, E. Arens, Z. Lian, Machine learning approaches to predict thermal demands using skin temperatures: Steady-state conditions, Building and Environment 114 (2017) 1 – 10. doi:https://doi.org/10.1016/j.buildenv.2016.12.005.
URL http://www.sciencedirect.com/science/article/pii/S036013231630484X

[22] T. Chaudhuri, D. Zhai, Y. C. Soh, H. Li, L. Xie, Thermal comfort prediction using normalized skin temperature in a uniform built environment, Energy and Buildings 159 (2018) 426 – 440. doi:https://doi.org/10.1016/j.enbuild.2017.10.098.
URL http://www.sciencedirect.com/science/article/pii/S0378778817327354

[23] J.-H. Choi, D. Yeom, Study of data-driven thermal sensation prediction model as a function of local body skin temperatures in a built environment, Building and Environment 121 (2017) 130 – 147. doi:https://doi.org/10.1016/j.buildenv.2017.05.004.
URL http://www.sciencedirect.com/science/article/pii/S0360132317301841

[24] A. Ghahramani, G. Castro, B. Becerik-Gerber, X. Yu, Infrared thermography of human face for monitoring thermoregulation performance and estimating personal thermal comfort, Building and Environment 109 (2016) 1 – 11. doi:https://doi.org/10.1016/j.buildenv.2016.09.005.
URL http://www.sciencedirect.com/science/article/pii/S0360132316303456

[25] M. Burzo, C. Wicaksono, M. Abouelenien, V. Perez-Rosas, R. Mihalcea, Y. Tao, Multimodal sensing of thermal discomfort for adaptive energy saving in buildings, iiSBE NET ZERO BUILT ENVIRONMENT (2014) 344.

[26] J. Ranjan, J. Scott, Thermalsense: Determining dynamic thermal comfort preferences using thermographic imaging, in: Proceedings of the 2016 ACM International Joint Conference on Pervasive and Ubiquitous Computing, UbiComp '16, ACM, New York, NY, USA, 2016, pp. 1212–1222. doi:10.1145/2971648.2971659.
URL http://doi.acm.org/10.1145/2971648.2971659

[27] B. Pavlin, G. Pernigotto, F. Cappelletti, P. Bison, R. Vidoni, A. Gasparella, Real-time monitoring of occupants' thermal comfort through infrared imaging: A preliminary study, Buildings 7 (1). doi:10.3390/buildings7010010.
URL http://www.mdpi.com/2075-5309/7/1/10

[28] A. C. Cosma, R. Simha, Thermal comfort modeling in transient conditions using real-time local body temperature extraction with a thermographic camera, Building and Environment 143 (2018) 36 – 47. doi:https://doi.org/10.1016/j.buildenv.2018.06.052.
URL http://www.sciencedirect.com/science/article/pii/S0360132318303962

[29] S.-E. Wei, V. Ramakrishna, T. Kanade, Y. Sheikh, Convolutional pose machines, in: CVPR, 2016, pp. 4724–4732. doi:10.1109/CVPR.2016.511.

[30] Center for Building Performance and Diagnostics, GSA workplace 2020 project technical report to the U.S. General Services Administration (2008).